ADVANCES IN ATMOSPHERIC SCIENCES, VOL. 31, SEPTEMBER 2014, 1181–1196

On the Blocking Flow Patterns in the Euro–Atlantic Sector: A Simple Model Study

LUO Dehai*[1,2] and YAO Yao[1,2]

[1]*Physical Oceanography Laboratory, College of Physical and Environmental Oceanography, Ocean University of China, Qingdao* 266100

[2]*Key Laboratory of Regional Climate-Environment for East Asia, Chinese Academy of Science, Beijing* 100029

(Received 25 September 2013; revised 18 January 2014; accepted 27 February 2014)

ABSTRACT

The flow patterns of Euro–Atlantic blocking events in winter are investigated by dividing the sector into three sub-regions: 60°–30°W (Greenland region); 20°W–30°E [eastern Atlantic–Europe (EAE) region]; and 50°–90°E (Ural region). It is shown that blocking events in winter are extremely frequent in the three sub-regions. Composite 500-mb geopotential height fields for intense and long-lived blocking events demonstrate that the blocking fields over Greenland and Ural regions exhibit southwest–northeast (SW–NE) and southeast–northwest (SE–NW) oriented dipole-type patterns, respectively, while the composite field over the EAE region exhibits an Ω-type pattern. The type of composite blocking pattern seems to be related to the position of the blocking region relative to the positive center of the climatological stationary wave (CSW) anomaly existing near 10°W.

The physical cause of why there are different composite blocking types in the three sub-regions is identified using a nonlinear multiscale interaction model. It is found that when the blocking event is in almost the same position as the positive CSW anomaly, the planetary-scale field can exhibit an Ω-type pattern due to the enhanced positive CSW anomaly. Nevertheless, a SW–NE (SE–NW) oriented dipole-type block can occur due to the reduced positive CSW anomaly as it is farther in the west (east) of the positive CSW anomaly. The total fields of blocking in the three regions may exhibit a meandering flow comprised of several isolated anticyclonic and cyclonic vortices, which resembles the Berggren-Bolin-Rossby meandering jet type.

Key words: blocking flow pattern, synoptic eddies, nonlinear multiscale interaction, climatological stationary wave anomaly

Citation: Luo, D. H., and Y. Yao, 2014: On the blocking flow patterns in the Euro–Atlantic sector: A simple model study. *Adv. Atmos. Sci.*, **31**(5), 1181–1196, doi: 10.1007/s00376-014-3197-1.

1. Introduction

Atmospheric blocking is a quasi-stationary, or slowly retrograde planetary-scale regime persisting for at least one week or more in mid-high latitudes (Berggren et al., 1949; Rex, 1950a, 1950b). In the Northern Hemisphere, blocking events are seen to occur frequently over the Pacific and Euro–Atlantic sectors (Lejenäs and Økland, 1983; Tibaldi and Molteni, 1990; Pelly and Hoskins, 2003; Barriopedro et al., 2006; Diao et al., 2006; Tyrlis and Hoskins, 2008). The genesis and persistence of blocking events over Europe has been recognized to result in extreme cold weathers in winter (Cattiaux et al., 2010; Buehler et al., 2011; Sillmann et al., 2011; de Vries et al., 2012) as well as summer heat waves and drought over Europe (Green, 1977; Trigo et al., 2005; Dole et al., 2011). Some studies have also examined the characteristics and impacts of Ural–Siberia blocking on downstream circulation and their impact on East Asian Winter Monsoon (Cheung et al., 2012, 2013). Thus, understanding the variability of blocking events has been an important research topic in the atmospheric science fields since blocking flow was first discovered.

The instantaneous field of a blocking flow in a total field is known to comprise several isolated anticyclonic and cyclonic vortices (Berggren et al., 1949; Rex, 1950a). However, the composite field of blocking events shows a dipole-type or an Ω-type pattern (McWilliams, 1980; Higgins and Schubert, 1994; Nakamura and Wallace, 1993). This hints that the blocking flow in a planetary-scale field is often either an Ω-type or a dipole-type pattern. It has been recognized that the shape of the planetary-scale blocking field is important for the path and regional variations of rapidly travelling synoptic eddies around the blocking region (Shutts, 1983; Higgins and Schubert, 1994; Yamazaki and Itoh, 2013), although there is a strong coupling between the planetary-scale blocking flow and synoptic-scale eddies. However, it is so far from clear under what condition the planetary-scale field of the block-

* Corresponding author: LUO Dehai
Email: ldh@mail.iap.ac.cn

ing flow can show an Ω-type or dipole-type pattern. The purpose of this paper is to try to investigate this problem, but we only examine the case of Euro–Atlantic blocking events in winter because blocking events are more frequent in the Euro–Atlantic sector than in the Pacific sector (Tibaldi and Molteni, 1990; Diao et al., 2006).

The paper is organized as follows. In section 2, the data and detecting method of blocking action are introduced. Using the blocking index of Tibaldi and Molteni (1990; TM), results on the regional features (frequency, intensity, and location) of Euro–Atlantic blocking events are presented in section 3 by dividing the Euro–Atlantic region into three subregions: 60°–30°W (Greenland region); 20°W–30°E [eastern Atlantic–Europe (EAE) region]; and 50°–90°E (Ural region). A simple nonlinear multiscale interaction (NMI) model is briefly described in section 4. In section 5, we use the NMI model to reveal the factors affecting the flow patterns of Euro–Atlantic blocking events. It is found that the existing position of the weak westerly wind of the North Atlantic jet stream is very important for the occurrence region of Euro–Atlantic blocking events. While the strengths of the mean zonal wind and storm track in the Atlantic basin can affect the intensity, duration and location of blocking events, the zonal position of the blocking anomaly occurring in the three regions relative to the positive climatological stationary wave (CSW) anomaly existing near 10°W is crucial for whether or not the planetary-scale blocking field exhibits an Ω-type or dipole-type pattern. Further discussion and conclusions are summarized in section 6.

2. Data and blocking detection method

2.1. *Data*

The dataset used in this study consists of daily multilevel height geopotential fields on a 2.5° × 2.5° grid from the National Centers for Environmental Prediction–National Center for Atmospheric Research (NCEP–NCAR) during the period from November 1950 to March 2012. In this study, winter is defined to be a time interval of five months from November to March. The seasonal cycle has been removed from the grid point fields. The Atlantic storm track (mean zonal wind) is defined as the winter mean of the 2.5–7-day eddy kinetic energy (EKE) (zonal wind) at 300 hPa that would exist without the blocking.

2.2. *Blocking detection method*

To identify the occurrence region of Euro–Atlantic blocking events, it is reasonable to use the bi-dimensional (2D) blocking index of Davini et al. (2012a, 2012b) to examine the blocking activity in the Euro–Atlantic region. This 2D index is an extension of the one-dimensional blocking index proposed by Tibaldi and Molteni (1990; TM), which is defined by calculating the daily 500-hPa geopotential height gradient at each longitude:

$$Z_{\rm S}(\lambda_0,\phi_0)=\frac{Z(\lambda_0,\phi_0)-Z(\lambda_0,\phi_{\rm S})}{\phi_0-\phi_{\rm S}}>0\ , \tag{1a}$$

$$Z_{\rm N}(\lambda_0,\phi_0)=\frac{Z(\lambda_0,\phi_{\rm N})-Z(\lambda_0,\phi_0)}{\phi_{\rm N}-\phi_0}<-10\ , \tag{1b}$$

$$Z_{\rm S2}(\lambda_0,\phi_0)=\frac{Z_{500}(\lambda_0,\phi_{\rm S})-Z_{500}(\lambda_0,\phi_{\rm S}-15)}{15}<-5\ , \tag{1c}$$

where $\phi_{\rm N}=\phi_0+15$; $\phi_S=\phi_0-15$; $\lambda_0(\phi_0)$ is the grid-point longitude (latitude) and ranges from longitude 0° to 360° (latitude 30°N to 75°N); and $Z(\lambda_0,\phi_0)$ is the daily 500-hPa geopotential height at the given grid point (λ_0,ϕ_0). Here, $Z_{\rm N}$ and $Z_{\rm S}$ represent the 500-hPa geopotential height gradients [unit: m (°lat)$^{-1}$] on the north and south sides of the grid point (λ_0,ϕ_0), respectively.

An instantaneous blocking (IB) event is identified if (1a) and (1b) is satisfied. Large-scale blocking is identified if IB event be extended for at least 15° of continuous longitude. A blocking event is defined if the large-scale blocking event occurs within a box with 10° of longitude and 5° of latitude around a given grid point for at least 5 days. Low-latitude blocking events are excluded if constraint $Z_{\rm S2}$ (1c) is satisfied here (Davini et al., 2012a, 2012b).

In the 2D blocking index, the blocking intensity is defined as (Wiedenmann et al., 2002; Davini et al., 2012a, 2012b):

$$B_{\rm I}(\lambda_0,\phi_0)=100\left[\frac{Z(\lambda_0,\phi_0)}{R(\lambda_0,\phi_0)}-1.0\right]\ , \tag{2a}$$

$$R(\lambda_0,\phi_0)=\frac{[Z_{\rm U}+Z(\lambda_0,\phi_0)]/2+[Z_{\rm D}+Z(\lambda_0,\phi_0)]/2}{2}\ , \tag{2b}$$

where $Z_{\rm U}$ and $Z_{\rm D}$ are the minimum of the $Z(\lambda_0,\phi_0)$ field within 60° upstream and downstream at the same latitude (ϕ_0) of the chosen point, and R is a measure of the size (wavelength) of the blocking flow (Wiedenmann et al., 2002). We may exclude very low-latitude blocking events and subtropical ridges in the Atlantic basin when the constraint condition (1d) is used. More details of this blocking index can be found in Davini et al. (2012a).

When $\phi_{\rm N}=80+\Delta,\phi_0=60+\Delta,\phi_{\rm S}=40+\Delta$ and $\Delta=-4$, 0 or 4 are used in Eqs. (1a) and (1b), Eqs. (1a)–(1c) define the TM index. In this case, the 2D blocking index is reduced to the TM index. In the 2D index, $B_{\rm I}(\lambda_0,\phi_0)$ is defined as the blocking intensity at a given grid point, (λ_0,ϕ_0), while the value of $Z_{\rm S}$ is defined as the blocking intensity in the TM index. Using the 2D index of Davini et al. (2012a, 2012b), we can obtain the spatial distribution of the blocking activity in the Euro–Atlantic sector. Through inspecting the horizontal distribution of the blocking frequency, it is likely to divide the occurrence region of Euro–Atlantic blocking events into several high blocking frequency sub-regions. In this case, the number of blocking cases occurring in these three subregions can be identified using the TM index.

3. Observational results

3.1. *Regional characteristics of Euro–Atlantic blocking events and their relationship with the North Atlantic jet stream and storm track*

We show the blocking frequency, intensity and duration of blocking events in the Euro–Atlantic sector during 1950–

2012 in Fig. 1 by using the 2D blocking index of Davini et al. (2012a, 2012b). The blocking frequency is defined as the percentage of blocked days with respect to total days in winter. It can be seen that there are three preferential occurrence regions of blocking events in the Euro–Atlantic sector: 60°–30°W (Greenland region); 20°W–30°E [eastern Atlantic–Europe (EAE) region]; and 50°–90°E (Ural region). The blocking events in the EAE region are most frequent but occur in a relatively low-latitude region. The Greenland blocking events occur in a relatively high-latitude region, but are less frequent than those in the EAE region. Meanwhile, the blocking events in the Ural region are least relative to those in the other two regions. The blocking intensity and duration exhibits similar features in the three sub-regions (Figs. 1b and c). To understand which factors dominate the preferential occurrence region of blocking events over the Euro–Atlantic sector, we show the winter mean zonal wind and EKE at 300 hPa during 1950–2012 in Fig. 2. It can be seen that the North Atlantic jet stream is distributed along the southwest–northeast (SW–NE) direction. In other words, the jet stream has a jet core along the SW–NE direction. A comparison with Fig. 1a shows that the occurrence regions of blocking events follow the spatial distribution of the jet core of the North Atlantic jet stream. The three preferential occurrence regions of Euro–Atlantic blocking events correspond to the existing regions of the weak westerly wind in the North Atlantic jet stream. This suggests that Euro–Atlantic blocking events occur only in the weak westerly wind regions of the North Atlantic jet stream. Although the winter mean EKE (Atlantic storm track) exhibits a spatial pattern similar to that of the North Atlantic jet stream (Fig. 2b), its spatial distribution along the west–east direction seems to be dominant.

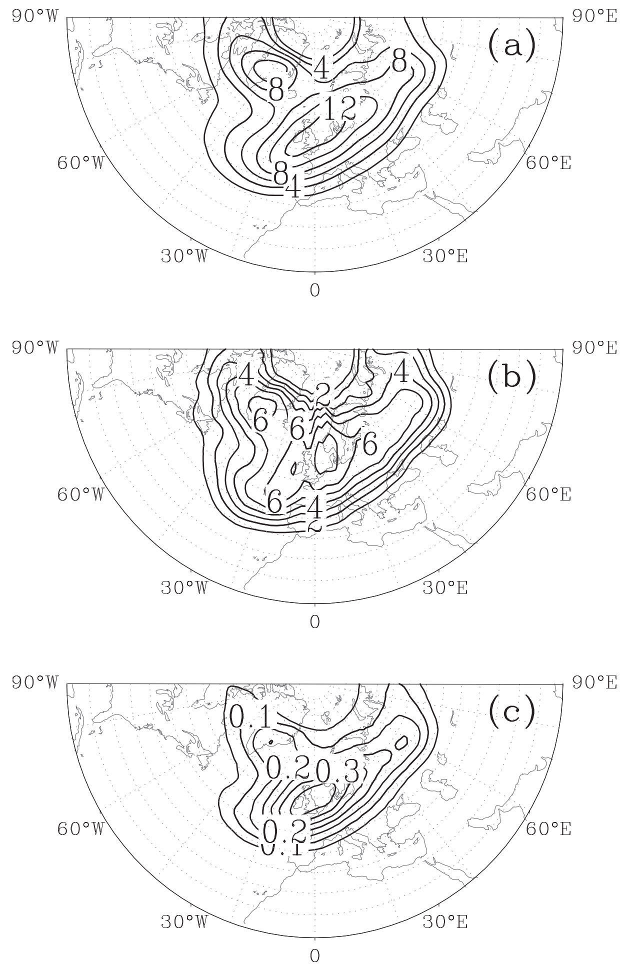

Fig. 1. Geographic distribution of the blocking (a) frequency, (b) intensity and (c) duration of blocking events in the Euro–Atlantic sector. Units are: (a) %, (b) non-dimensional, and (c) day.

3.2. *Different blocking flow patterns in the three sub-regions*

The number, duration and intensity of blocking events are shown in Table 1. We find that the blocking events in the EAE region occur most frequently, which is consistent with the distribution of blocking frequency in Fig. 1. The strong and long-lived blocking events in the Greenland region seem to have the strongest intensity and longest duration compared to the EAE and Ural regions. This can be explained by the distribution of winter mean EKE in Fig. 2, in which the maximum core of the EKE (westerly wind) is located closest to the Greenland region. The persistent forcing of the EKE may lead to a long-lived and intense blocking process. Moreover, the duration of blocking events with strong intensity ($Z_S > 4$) is usually shorter than blocking events with relatively weaker intensity ($Z_S > 0$), as shown in Table 1.

Table 1. Number, mean duration and mean intensity of blocking events for the duration of $\geqslant 7$ days and $\geqslant 3$ days with strong ($Z_S > 4.0$) and weak ($Z_S > 0.$) intensity in the three sub-regions. The three values in each cell separated by "/" refer, from left to right, to the number, mean duration, and mean intensity.

Sub-region	Duration $\geqslant 3$ days		Duration $\geqslant 7$ days	
	$Z_S > 0$	$Z_S > 4$	$Z_S > 0$	$Z_S > 4$
Greenland	170/7.3/4.8	100/6.4/8.3	75/11.1/6.2	33/10.2/10
EAE	353/8.9/4.1	232/6.4/7.0	197/12.5/4.9	86/9.8/7.9
Ural	147/7.1/3.0	77/6.1/6.4	65/10.9/4.1	23/9.8/7.7

Because intense and long-lived blocking events are more important for extreme cold events in winter (Buehler et al., 2011; de Vries et al., 2012) and heat waves in summer (Dole et al., 2011), it is useful to examine what factors dominate the flow patterns of relatively intense and long-lived blocking events. Therefore, we only consider two cases here. The first one is that Z_S in the TM index has a larger positive value that corresponds to intense blocking events, and the other is that blocking events have longer durations. For the first case, without the loss of generality, $Z_S > 4.0$ is chosen in the TM index so that blocking events considered in this paper are relatively strong. For long-lived blocking events, their durations are defined to be at least seven days as an example.

For comparison, we show the composites of 500-hPa geopotential height fields for all blocking days in the three sub-regions in Fig. 3 for two cases of $Z_S > 0$ and $Z_S > 4.0$.

It is noted that for blocking events with $Z_S > 0$ the composite fields exhibit an Ω-type pattern, but have different spatial patterns. In particular, the blocking type in the Ural region seems to be a typical Ω-type pattern. However, for blocking events with $Z_S > 4.0$, the composite fields in the Greenland and Ural regions tend to become a dipole-type blocking even though the low pressure to the south of the blocking anticyclone is relatively weak. An interesting result is that the composite blocking field in the EAE region still exhibits an Ω-type pattern. This raises an interesting problem why the planetary-scale fields of intense blocking events have dipole-type patterns in the Greenland and Ural regions, but an Ω-type pattern in the EAE region. We investigate this problem in detail in this paper.

We show the composite of daily 500-hPa geopotential height fields for blocking events during their total life cycles in the Greenland, EAE and Ural regions in Fig. 4 for intense blocking events with $Z_S > 4.0$, where lag(0) denotes the day on which the strongest amplitude of a blocking event occurs. It is found that for Greenland blocking events, a weak blocking ridge is located in the region from 30°W to 0° at lag(−6). This weak ridge can be amplified into a typ-

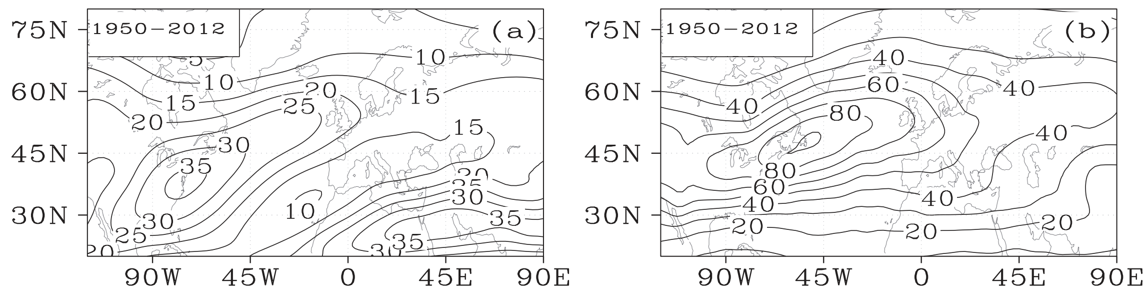

Fig. 2. (a) Winter mean zonal wind and (b) eddy kinetic energy (EKE) at 300 hPa during 1950–2012. Units are: (a) m s^{-1} and (b) m^2 s^{-2}.

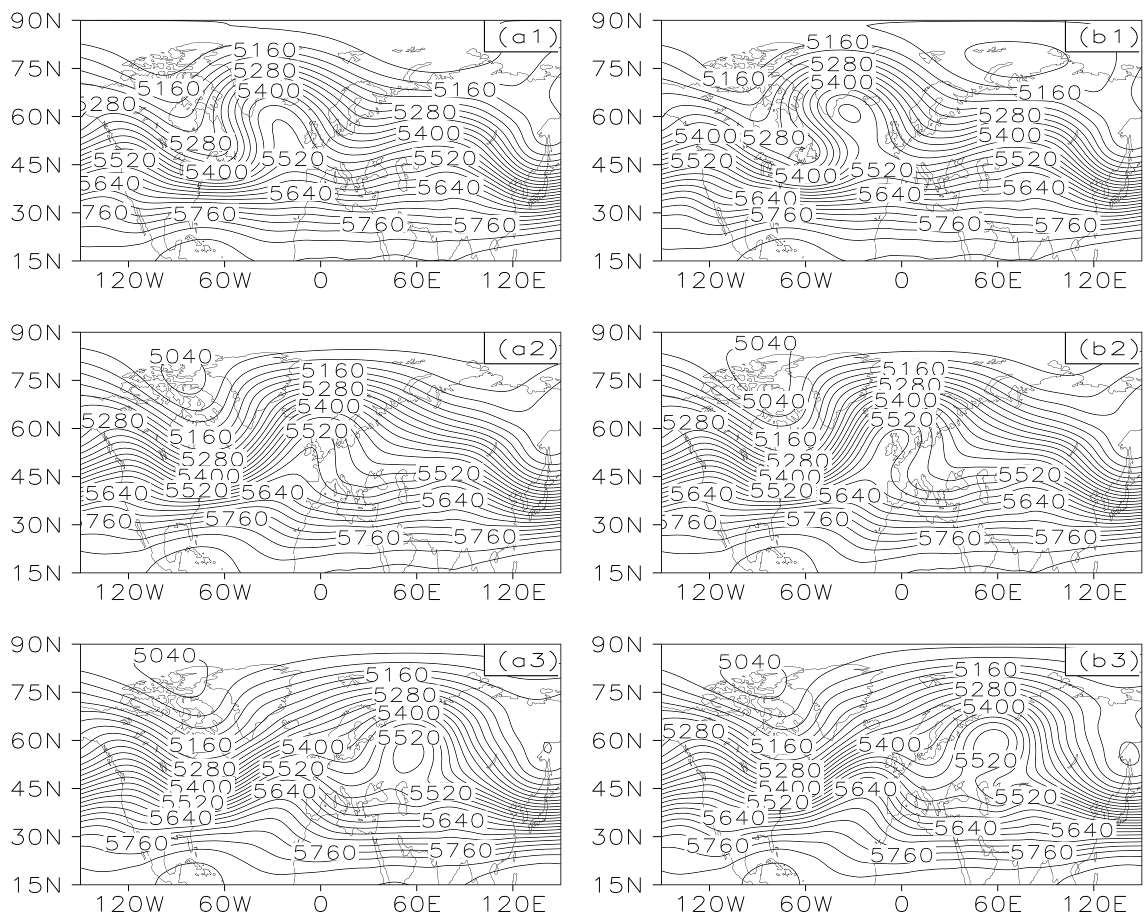

Fig. 3. Composites of 500-mb geopotential height fields in the (a1, b1) Greenland, (a2, b2) EAE, and (a3, b3) Ural regions for different values of blocking intensity, Z_S: (a) $Z_S > 0$; (b) $Z_S > 4.0$. Units: m.

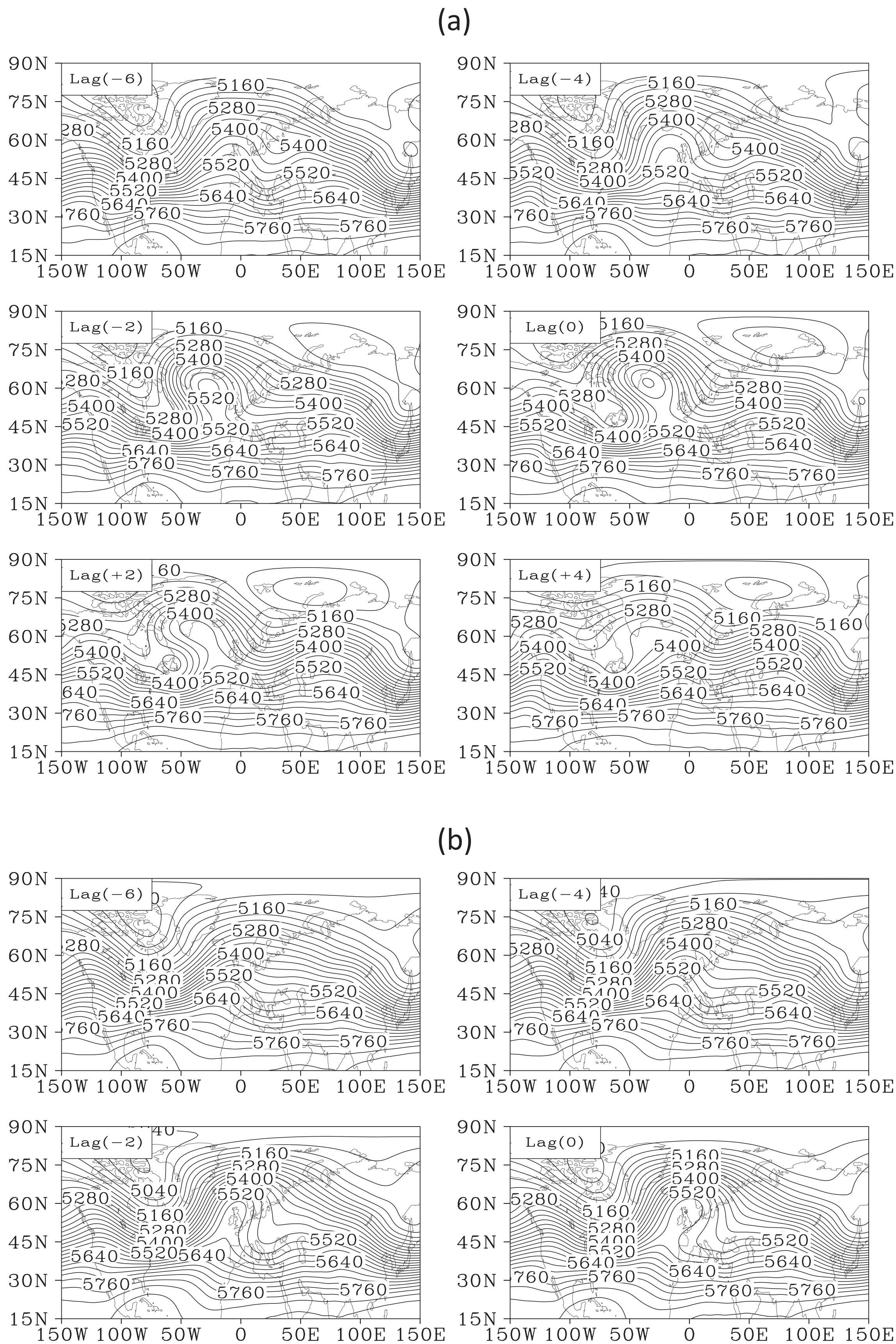

Fig. 4. Time sequences of the composite 500-mb geopential height fields for blocking events in (a) Greenland, (b) EAE and (c) Ural regions for the blocking intensity $Z_S > 4.0$. The units are m.

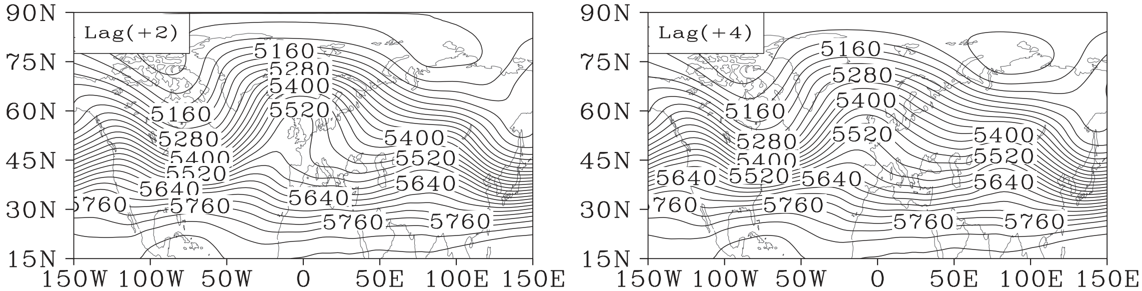

(c)

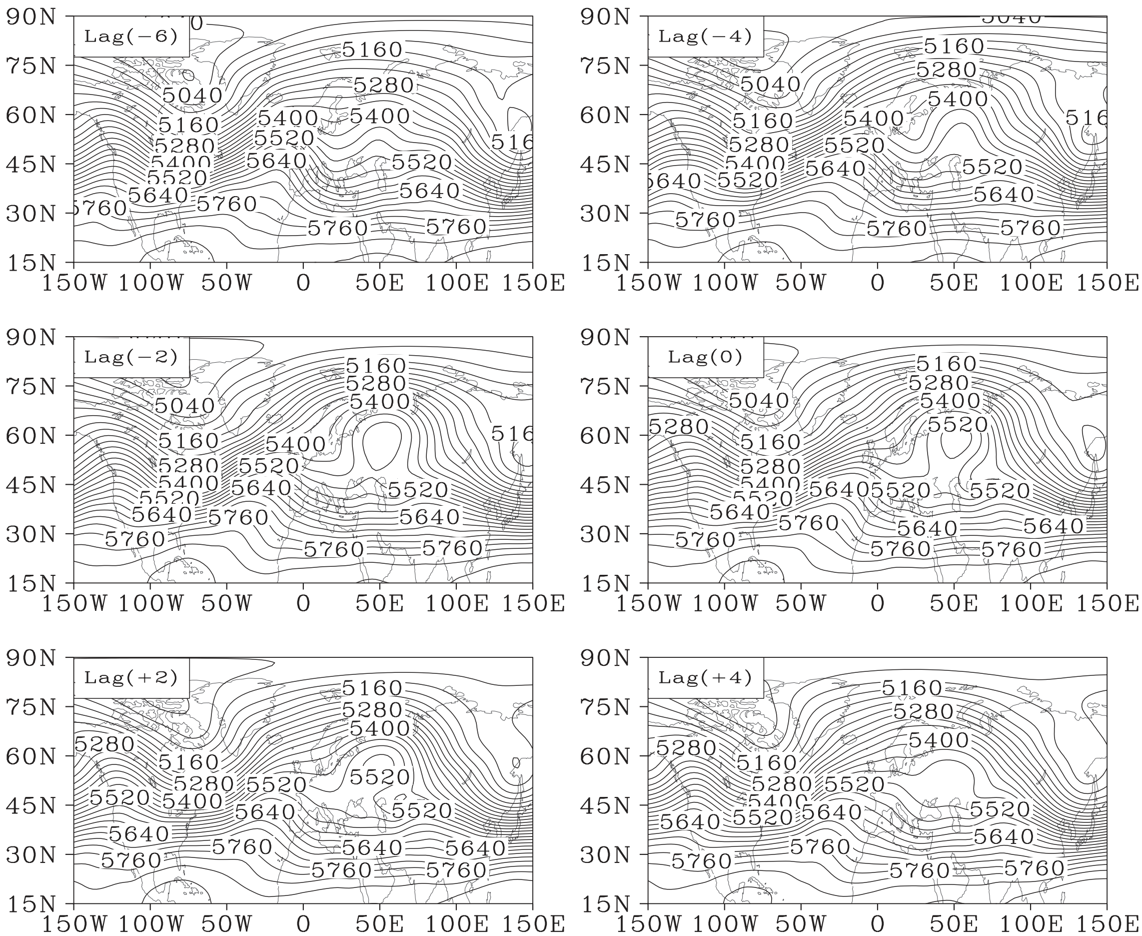

Fig. 4. (continued)

ical blocking pattern that exhibits a SW–NE-oriented dipole block pattern in the mature stage [lag(−2) to lag(+2)] (Fig. 4a). Such a dipole block is hereafter referred to as the SW–NE-type dipole block. For blocking events in the Ural region, a weak diffluent flow as a weak blocking ridge is located near 60°E at lag(−6), which is reinforced into a blocking flow by upstream synoptic eddies (Shutts, 1983; Yamazaki and Itoh, 2013). This blocking pattern can exhibit an obvious southeast–northwest (SE–NW) oriented dipole pattern during the period from lag(−2) to lag(+2) even though the low pressure to the south of the blocking anticyclone is relatively weak (Fig. 4c). Such a dipole block is hereafter called the SE–NW-type dipole block. Furthermore, an interesting point is that the composite field of blocking events in the EAE region shows an Ω-type blocking pattern (Fig. 4b). For long-lived blocking events in the three sub-regions, similar results are found (not shown). In the following sections, we examine why the composite fields of intense and long-lived blocking events in the three sub-regions of the Euro–Atlantic sector can exhibit different blocking patterns.

3.3. *The flow pattern of the composite blocking field and its relationship with the longitudinal position of the climatological stationary wave anomaly in winter*

To understand the physical cause of why the composite fields of intense and long-lived blocking events exhibit different flow patterns in the Greenland, EAE and Ural regions, we show the winter mean stationary wave anomaly during 1950–2012 in Fig. 5. Because the stationary wave anomaly obtained here is a long-term average, it is considered to be a climatological stationary wave (CSW) anomaly induced by the land–sea configuration (topography). It is seen from a comparison with Figs. 3 and 4 that the Greenland (Ural) blocking events are in the west (east) of the positive CSW anomaly, but the position of the blocking occurrence in the EAE region is almost the same as the CSW anomaly. Thus, it is concluded that, along with the variations of the North Atlantic jet stream and storm track, the longitudinal position of the occurrence region of the blocking events relative to the positive CSW anomaly is important for different flow patterns of the composite blocking fields in the Greenland, EAR and Ural regions. The physical cause of these different blocking patterns is examined using a nonlinear multiscale interaction (NMI) model, as described briefly in the following section.

In the next section, the CSW anomaly is assumed to be approximated as a stationary Rossby wave with a monopole meridional pattern induced by the wavenumber-two topography (Charney and DeVore, 1979) because its dominant monopole pattern exhibits a wavenumber-two distribution.

4. Nonlinear multi-scale interaction model of blocking events

Although baroclinic processes might play a certain role in the formation of blocking anticyclones (White and Clark, 1975), the barotropic process of the blocking establishment seems to be dominant (Colucci, 1985). In this case, it is reasonable to use an equivalent barotropic model to examine our problem (Charney and DeVore, 1979). Here, we still use the wavenumber-two topography as an approximation of the land–sea configuration in mid-high latitudes, as in Charney and DeVore (1979). However, although there is an intense jet stream in the Atlantic basin, the mean westerly wind in the occurrence regions of Euro–Atlantic blocking events is relatively weak and uniform (Fig. 2a). In this case, the mean zonal wind in the blocking region can be assumed to be uniform.

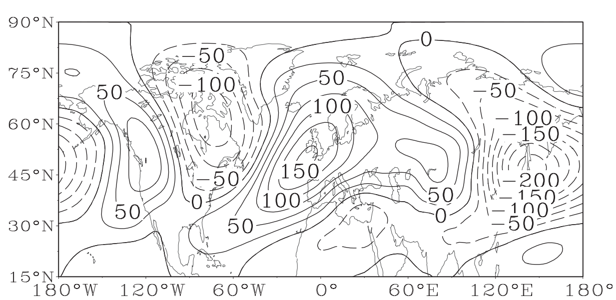

Fig. 5. Horizontal distribution of the climatological stationary wave (CSW) anomaly at 500 hPa in winter during 1950–2012. Units: m.

Since synoptic eddies play an important role in the genesis of blocking events (planetary-scale) in the Euro–Atlantic sector (Berggren et al., 1949; Holopainen and Fortelius, 1987), it is reasonable to split the total streamfunction into three parts: basic flow ($-u_0 y, u_0$ is the uniform westerly wind); planetary-scale as a blocking scale (ψ); and the synoptic scale (ψ'). Then, under the scale separation assumption, the nondimensional equations of the interaction between the blocking flow and synoptic eddies in a beta plane channel with width L_y can be easily obtained as (Luo, 2005; Luo and Cha, 2012):

$$\left(\frac{\partial}{\partial t}+u_0\frac{\partial}{\partial x}\right)(\nabla^2\psi - F\psi)+J(\psi,\nabla^2\psi+h)+ (\beta+Fu_0)\frac{\partial\psi}{\partial x}+u_0\frac{\partial h}{\partial x}=-J(\psi',\nabla^2\psi')_{\mathrm{P}}\,, \tag{3a}$$

$$\left(\frac{\partial}{\partial t}+u_0\frac{\partial}{\partial x}\right)(\nabla^2\psi' - F\psi')+(\beta+Fu_0)\frac{\partial\psi'}{\partial x} =-J(\psi',\nabla^2\psi+h)-J(\psi,\nabla^2\psi')+\nabla^2\psi_{\mathrm{s}}^*\,, \tag{3b}$$

where $F=(L/R_{\mathrm{d}})^2$; L and R_{d} are the characteristic length and radius of Rossby deformation, respectively; The subscript P represents the planetary-scale component whose zonal wavenumber is close to that of the blocking flow. h is a topographic parameter; and $\nabla^2\psi_{\mathrm{s}}^*$ is designed as a synoptic-scale wave-maker or synoptic-scale vorticity source. That is to say, the local synoptic-scale eddies maintained by $\nabla^2\psi_{\mathrm{s}}^*$ are organized to represent an Atlantic storm track that would exist without blocking events. The other notations can be found in Luo (2005) and Luo and Cha (2012).

Here, to reflect the effect of the different mean zonal wind strength on blocking events in different regions, we suppose $u_0=u_C+\Delta u, u_C=\beta/(k^2+m^2)$ which represents a critical westerly wind and $|\Delta u|\ll u_C$, where $k=2k_0, k_0=1/[6.371\cos(\phi_0)]$ and $m=-2\pi/L_y$ are the zonal and meridional wavenumbers of the blocking event, respectively. Here, $\Delta u>0$ ($\Delta u<0$) corresponds to an enhanced (reduced) background westerly wind prior to the block onset. Similar to Charney and DeVore (1979), we assume that the two-wave topography is of the form $h=h_0\exp[ik(x+x_{\mathrm{T}})]\sin\left(\frac{m}{2}y\right)+\mathrm{cc}$, where $k=2k_0$ is the zonal wavenumber of the wavenumber-two topography, $i=\sqrt{-1}$ and h_0 is the amplitude, x_{T} is the zonal position of a topographic trough, and cc denotes the complex conjugate of its preceding term.

The analytical solutions of the total atmospheric streamfunction (Ψ_{tot}) of a blocking event in a fast varying form can be obtained as (Luo, 2005; Luo and Cha, 2012):

$$\Psi_{\mathrm{tot}}=-u_0y+\psi+\psi'=\psi_{\mathrm{P}}+\psi'\,, \tag{4a}$$

$$\psi_{\mathrm{P}}=-u_0y+\psi\approx\psi_w+\psi_m\,, \tag{4b}$$

$$\psi_w=-u_0y+\psi_A+\psi_C\,, \tag{4c}$$

$$\psi_A = B\sqrt{\frac{2}{L_y}}\exp(ikx)\sin(my) + \mathrm{cc}\,, \tag{4d}$$

$$\psi_C = h_A h_0 \exp[ik(x+x_\mathrm{T})]\sin\left(\frac{m}{2}y\right) + \mathrm{cc}\,, \tag{4e}$$

$$\psi_m = \psi_{m1} + \psi_{m2}\,, \tag{4f}$$

$$\psi_{m1} = -|B|^2\sum_{n=1}^{\infty} q_n g_n \cos(n+1/2)my\,, \tag{4g}$$

$$\psi_{m2} = -h_0 h_A\sqrt{\frac{2}{L_y}}(Be^{-ikx_\mathrm{T}} + B^* e^{ikx_\mathrm{T}})\sum_{n=1}^{\infty}\tilde{q}_n(3a_n - b_n)\cos(nmy)\,, \tag{4h}$$

$$\psi' \approx \varepsilon^{3/2}(\tilde{\psi}'_0 + \varepsilon\tilde{\psi}'_1) = \psi'_1 + \psi'_2\,, \tag{4i}$$

$$\psi'_1 = \varepsilon^{3/2}\tilde{\psi}'_0 = f_0(x)\{\exp[i(\tilde{k}_1 x - \tilde{\omega}_1 t)] + \alpha\exp[i(\tilde{k}_2 x - \tilde{\omega}_2 t)]\}\sin\left(\frac{m}{2}y\right) + \mathrm{cc}, \tag{4j}$$

$$\begin{aligned}\psi'_2 = &-\frac{m}{4}\sqrt{\frac{2}{L_y}}Bf_0(x)\sum_{j=1}^{2}Q_j\alpha_j\exp\{i(\tilde{k}_j + k)x - \tilde{\omega}_j t]\}\left[p_j\sin\left(\frac{3m}{2}y\right) + r_j\sin\left(\frac{m}{2}y\right)\right]\\ &+\frac{m}{4}\sqrt{\frac{2}{L_y}}B^* f_0(x)\sum_{j=1}^{2}Q_j\alpha_j\exp\{i(\tilde{k}_j - k)x - \tilde{\omega}_j t]\}\left[s_j\sin\left(\frac{3m}{2}y\right) + h_j\sin\left(\frac{m}{2}y\right)\right]\\ &-\frac{m}{4}f_0(x)h_0\sum_{j=1}^{2}\pi_j\alpha_j\exp\{i(\tilde{k}_j + k)x + kx_\mathrm{T} - \tilde{\omega}_j t]\}\sin(2my)\\ &-\frac{m}{4}f_0(x)h_0\sum_{j=1}^{2}\sigma_j\alpha_j\exp\{i(\tilde{k}_j - k)x - kx_\mathrm{T} - \tilde{\omega}_j t]\}\sin(2my) + \mathrm{cc}\,,\end{aligned} \tag{4k}$$

where $i = \sqrt{-1}$; $\alpha_1 = 1$; $\alpha_2 = \alpha = -1$; B^* is the complex conjugate of B, which represents the complex amplitude of the blocking anomaly, ψ_A; $h_A = -1/[\beta/u_C - (k^2 + m^2/4)]$, $\tilde{k}_j = 10k_0 + (-1)_j 0.75k_0$, and $\tilde{\omega}_j$ $(j = 1,2)$ are the zonal wavenumbers of each component of the synoptic eddies and their corresponding frequencies; $f_0(x) = a_0\exp[-\mu\varepsilon^2(x + x_0)^2]$ denotes the spatial distribution of the eddy amplitude for $\mu > 0$; a_0 is the maximum eddy strength on the upstream side of the Atlantic basin located at $x = -x_0$; and the other coefficients and notation can be found in Luo (2005), Luo and Cha (2012).

The temporal evolution of the blocking amplitude, B, is described by an eddy-forced nonlinear Schrödinger-like equation:

$$i\left(\frac{\partial B}{\partial t} + C_g\frac{\partial B}{\partial x}\right) + \lambda\frac{\partial^2 B}{\partial x^2} + \delta|B|^2 B + \tilde{\alpha}h_0^2(B + B^* e^{i2kx_\mathrm{T}}) + \Delta u\Gamma B + Gf_0^2\exp[-i(\Delta kx + \Delta\omega t)] = 0, \tag{5}$$

where $\Gamma = -k(k^2 + m^2)/(k^2 + m^2 + F)$, and the other notation and coefficients can be found in Luo and Cha (2012).

In this paper, the NMI model is used to examine the problem outlined above. The numerical method used to solve Eq. (5) is similar to that used in Luo (2005). It is possible to predict the temporal evolution of planetary-and synoptic-scale fields of a blocking event provided the initial pattern of the planetary-scale field in a blocking flow as well as the synoptic-scale eddies prior to the blocking onset are given. Unless otherwise stated, $B(x,0) = 0.4$ is chosen as the initial amplitude of the planetary-scale field of a blocking flow. Here, it should be noted that the synoptic-scale eddies have been assumed to have a potential that drives a blocking flow (Luo, 2005). This is a precondition of the blocking onset.

5. Theoretical results

5.1. *Parameter choices*

In this paper, the fixed basic parameters of atmospheric motions are chosen to be the same as in Luo and Cha (2012, their Table 1), but the varying of parameters h_0, x_0 and x_T is allowed. We show the stationary wave anomaly, ψ_C, induced by the wavenumber-two topography with a monopole meridional pattern in Fig. 6a for $h_0 = 0.4$ and $x_\mathrm{T} = 0$, and synoptic-scale eddies, ψ'_1, at $t = 0$ in Fig. 6b for $a_0 = 0.17$ and $x_0 = 2.87/2$. In this figure, only anomaly fields in the zonal domain with one wavelength $(-5.74 \leqslant x \leqslant 5.74)$ are plotted. It is noted that the idealized stationary wave anomaly, ψ_C, resembles the CSW anomaly, as seen in Fig. 5 (Fig. 6a), while the eddy anomaly field in Fig. 6b can be approximated as synoptic eddies in the Atlantic storm track. Varying the value of h_0 and x_T can represent the different amplitude and zonal position of the CSW anomaly. Thus, $x_\mathrm{T} > 0$ and $x_\mathrm{T} < 0$ must be required to represent that the initial blocking flow is

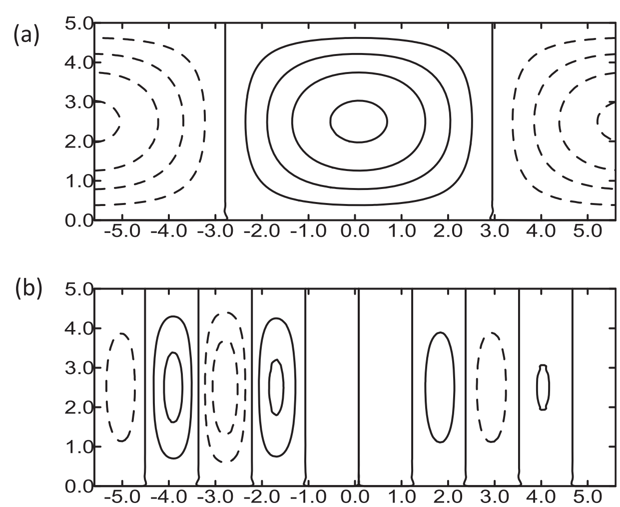

Fig. 6. (a) The stationary wave anomaly field induced by a wavenumber-two topography for $h_0 = 0.4$ and $x_\mathrm{T} = 0$ (CI = 0.2), and (b) the initial field ($t = 0$) of synoptic eddies for $a_0 = 0.17$ and $x_0 = 2.87/2$ (CI = 0.1).

in the east (west) of the positive CSW anomaly because the center of the initial blocking flow is always fixed at $x = 0$. On the other hand, the excited blocking event can be located in the EAE region for a value of $x_T > 0$ being not large because the intensified blocking anomaly, ψ_A, undergoes a westward shift due to the role of synoptic eddies. This assumption is acceptable because blocking events originate from Northern Europe (Sung et al., 2011). Since the amplitude of the positive CSW anomaly in the Greenland (Ural) region is weak relative to that in the EAE region, the value of h_0 should be chosen to be smaller. Moreover, because the blocking events are closer to the existing region of strongest synoptic eddies in the western Atlantic basin than those in the EAE and Ural regions, on this occasion, x_0 in the Greenland region should be chosen as a smaller value compared to those in the other two regions. In this case, we can consider three types of parameter settings as blocking parameters in the three regions: $(h_0 = 0.2, x_0 = 2.87/4, x_T = -1.5)$ over the Greenland region; $(h_0 = 0.5, x_0 = 2.87/2, x_T = 1.5)$ over the EAE region; and $(h_0 = 0.2, x_0 = 2.87, x_T = 2.5)$ over the Ural region.

5.2. *Blocking types and their relationship with the longitudinal position of the CSW anomaly*

We show the planetary-and synoptic-scale fields, and their total field of blocking events in the Greenland, EAE and Ural regions in Fig. 7 for $\Delta u = 0$ and $a_0 = 0.17$. It is clear that for the blocking parameters in the Greenland region the planetary-scale field of the eddy-driven blocking flow can exhibit a SW–NE-oriented dipole-type (SW–NE-type dipole) pattern with the blocking intensification (Fig. 7a) similar to the observed blocking pattern over Greenland, as shown in Fig. 4a, as well as the synoptic-scale eddies being split into two branches around the blocking region whose asymmetry is relatively north–south-oriented. The total field is found to bear a striking resemblance to the meandering jet-like blocking flow first observed by Berggren et al. (1949; BBR hereafter) and also noted by Rex (1950a). Such a blocking flow is hereafter referred to as BBR-type blocking. This suggests that the total field of the blocking event can generally exhibit a BBR-type blocking if it is excited by synoptic-scale eddies upstream of the blocking region. Because the process of the blocking formation corresponds to the northward (southward) shift of intensified warm (cold) air or anticyclones (cyclones) in the total field, as shown in Fig. 7, where the red (blue and green) denotes warm (cold) air, many investigations have suggested that blocking events arise from the cyclonic wave breaking (CWB) of synoptic eddies (Benedict et al., 2004; Franzke et al., 2004; Woollings et al., 2008). In the EAE region, the planetary-scale field of the formed blocking events has an Ω-type pattern resembling the observed one in Fig. 4b (7b). At the same time, it is seen that synoptic eddies on the north side of the blocking region become dominant due to the feedback of the intensified Ω-type blocking. This theoretical finding is supported by the observational evidence of Higgins and Schubert (1994), who noted that synoptic eddies undergo a marked northward deflection once an Ω-type blocking is formed in the Pacific basin. In the Ural region, the planetary-scale field of the eddy-driven blocking flow exhibits a SE–NW oriented dipole-type (SE–NW-type dipole) pattern even though the low pressure to the south of the anticyclone is relatively weak (Fig. 7c). In this case, two branches of synoptic eddies that are almost the same are still seen around the blocking region, and the BBR-type pattern of the blocking flow is also evident in the total field. Since the eddy-driven blocking flow obtained from this NMI model corresponds to more intense and persistent blocking events, the investigation made here suggests that the planetary-scale fields of intense and persistent blocking events can indeed exhibit a SW–NE-type dipole, Ω-type, and SE–NW-type dipole blocking pattern in the Greenland, EAE and Ural regions, even though they are produced by synoptic eddies upstream of the blocking region.

On the other hand, if the mean westerly wind is weaker (stronger), i.e., if $\Delta u < 0$ $(\Delta u > 0)$, blocking events are promoted (suppressed) (not shown). Thus, to some extent, this explains why Euro–Atlantic blocking events occur mainly in the weak westerly wind region of the North Atlantic jet stream.

5.3. *Sensitivity of blocking types to the zonal position of synoptic eddies.*

To understand whether the longitudinal position of the strongest region of synoptic eddies affects the flow patterns of the planetary-scale fields of blocking events in the Greenland, EAE and Ural regions, we consider the same parameters as in Fig. 7 except for the value of x_0. We show the planetary-scale fields of blocking events on day 9 in Figs. 8ai–ci $(i = 1-4)$ for $x_0 = 0, x_0 = 2.87/4, x_0 = 2.87/2$ and $x_0 = 1.5 \times 2.87/2$ in the Greenland, EAE and Ural regions, where day 9 is the strongest stage of the blocking event. It can be seen that the flow patterns of planetary-scale blocking fields in the Greenland, EAE and Ural regions are insensitive to the zonal position of the Atlantic storm track relative to blocking events over the three sub-regions in addition to the blocking intensity and duration. However, a dipole-type block is more easily established in the three sub-regions if synoptic eddies in the Atlantic storm track are so intense that the amplification of the dipole anomaly, ψ_A, is dominant (not shown).

5.4. *Physical cause of different flow patterns of planetary-scale blocking fields in different regions*

In this sub-section, we provide a theoretical explanation for why the planetary-scale fields of Euro–Atlantic blocking events can exhibit different blocking flow patterns in different regions. The flow patterns of the planetary-scale fields of the blocking events in the Greenland, EAE and Ural regions can in fact be explained in terms of the analytical solution of the planetary-scale blocking field of the form

$$\psi_P = -u_0 y + \psi \approx -u_0 y + \psi_A + \psi_C + \psi_m. \quad (6)$$

As described by Eqs. (4f)–(4h), because ψ_m represents the mean zonal flow and its form is independent of the sign of y,

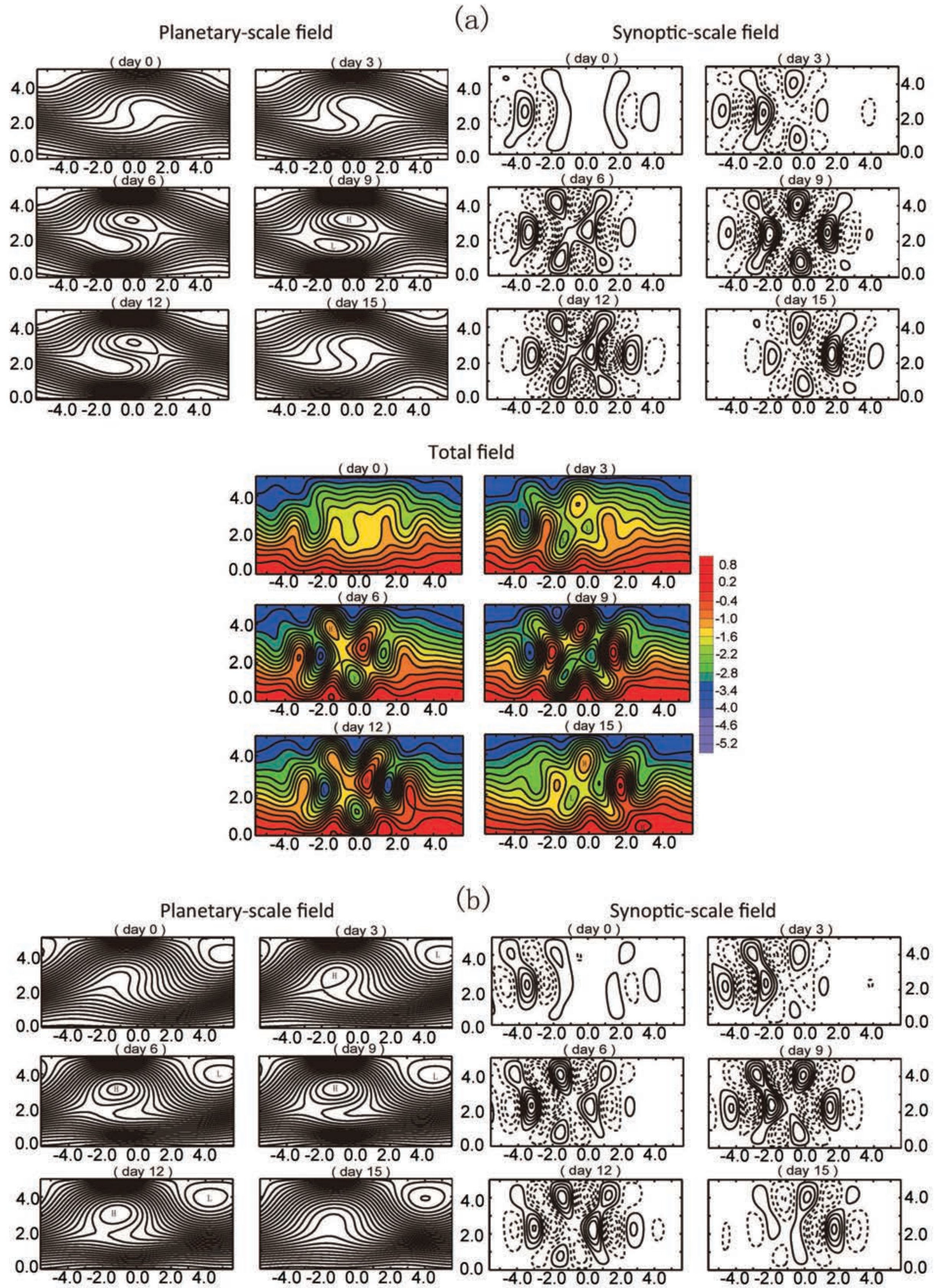

Fig. 7. Instantaneous planetary-(CI = 0.15) and synoptic-scale (CI = 0.3) fields and their total fields (CI = 0.3) of a blocking event obtained from the NMI model in the (a) Greenland, (b) EAE and (c) Ural regions.

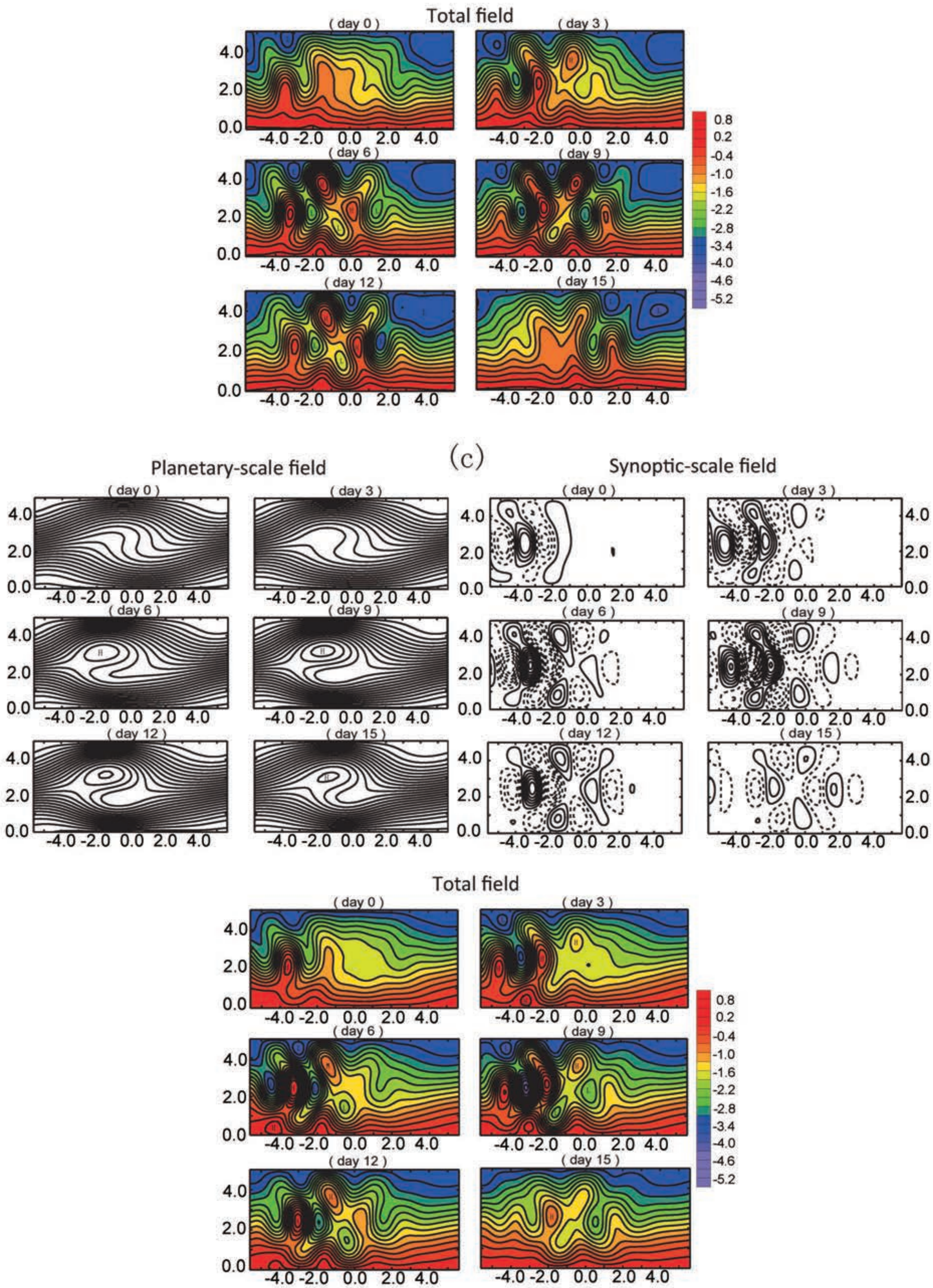

Fig. 7. (continued)

the flow patterns of the blocking field should be dominated by the relative strength of the dipole blocking anomaly, ψ_A, and the CSW anomaly, ψ_C. In particular, in the absence of the CSW anomaly, ψ_C, the planetary-scale blocking field, ψ_P,

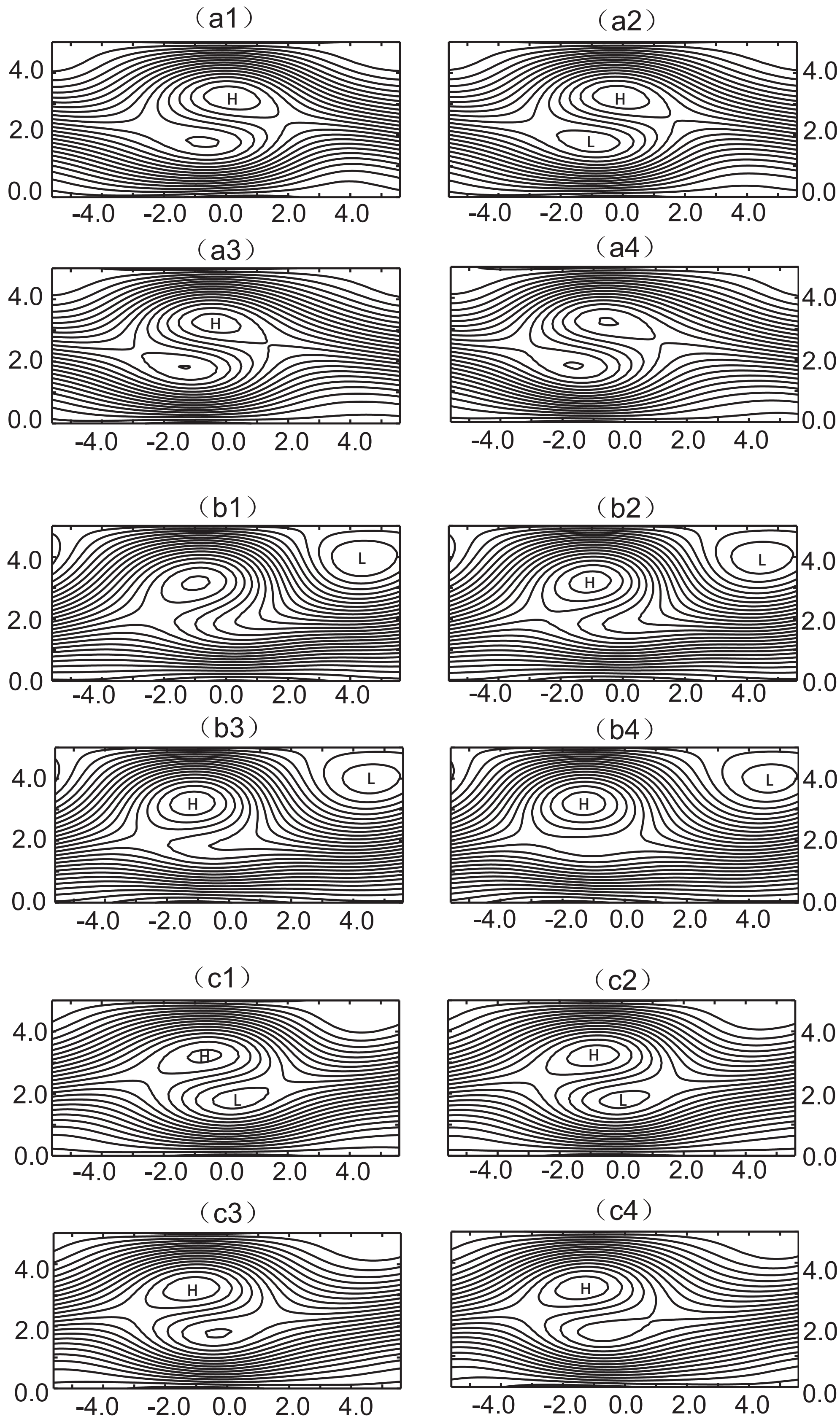

Fig. 8. Planetary-scale fields (CI = 0.3) of blocking events on day 9 in the (a*i*) Greenland, (b*i*) EAE and (c*i*) Ural regions (CI = 0.15), in which $i = 1$–4, denoting $x_0 = 0, x_0 = 2.87/4, x_0 = 2.87/2$, and $x_0 = 1.5 \times 2.87/2$, respectively.

can have a dipole-type pattern in that ψ_A (ψ_C) has a dipole (monopole) meridional pattern. If there is a strong positive ψ_C anomaly in the blocking region, the ψ_P field can exhibit an Ω-type pattern. In contrast, an asymmetric dipole block can occur when the positive ψ_C anomaly is weaker. In both the Greenland and Ural regions, an asymmetric dipole-type block can be easily established because there are weaker positive CSW anomalies in the two regions. However, Ω-type blocking patterns in the EAE region seem to be dominant due to the role of the enhanced positive CSW anomaly in the blocking area.

As revealed by Luo (2005), the eddy-amplified blocking dipole undergoes a marked retrograde drift with the blocking intensification. The retrogression of the amplified dipole anomaly, ψ_A, away from (approaching toward) the positive CSW anomaly can cause the SW–NE (SE–NW) orientation of the dipole blocking pattern in a planetary-scale field. This provides an explanation for why the blocking patterns have different spatial patterns in the Greenland, EAE and Ural regions. The results are also tenable in the Pacific basin (not shown).

6. A blocking case and idealized schematics of typical blocking patterns

To see how the total fields of observed blocking events evolve during the course of their existence, here we present a blocking case occurring in the Euro–Atlantic sector. The instantaneous 500-mb geopotential height fields of a blocking event occurring during 6–20 December 2012 are shown in Fig. 9. We find that a meandering jet-like blocking flow can form due to the interaction of a planetary-scale ridge with synoptic eddies, which looks like the BBR-type block first noted by Berggren et al. (1949) and then by Rex (1950a). As the total field on 10 or 12 December 2012 shows, there are three isolated anticyclonic vortices and three cyclonic vortices within the blocking region. If we can detect such a blocking pattern in an unfiltered field, it can be concluded that synoptic eddies play a key role in the genesis of the BBR-type block (Shutts, 1983; Holopainen and Fortelius, 1987). A comparison with the results from the NMI model indicates that the BBR-type block can be better captured by our NMI model (Fig. 7).

According to the observational and theoretical results presented above, several idealized flow patterns of blocking events in the Euro–Atlantic sector can be summarized and shown in Fig. 10. Although Figs. 10a–c reflect the blocking patterns in the Greenland, EAE and Ural regions, their total fields always look similar to the BBR-type blocking flow in Fig. 10d. However, if synoptic eddies, ψ', are relatively weak during the course of a blocking event, the total field of the blocking flow can also exhibit one of three patterns in Figs. 10a–c due to $\psi' \approx 0$. Of course, the strength of the mean zonal wind as well as the location and intensity of the Atlantic storm track can affect the intensity and location of isolated anticyclonic and cyclonic vortices coexisting within the blocking region. However, their basic characteristics are similar (not shown).

Many mechanisms have been proposed to account for how synoptic eddies drive a blocking flow (Shutts, 1983; Haines and Marshall, 1987; Luo, 2005; Yamazaki and Itoh, 2013). Shutts (1983) suggested that the eddy straining in the north–south direction tends to maintain a blocking dipole against the dissipation. Yamazaki and Itoh (2013) proposed that vortex–vortex interaction is responsible for the maintenance of the blocking dipole or anticyclone. However, Luo (2005) found that the spatial pattern of $-J(\psi_1', \nabla^2\psi_1')_{\mathrm{P}}$ prior to the block onset is crucial for whether or not a dipole blocking can be established. In this paper, because our emphasis has been to reveal the physical cause of different blocking patterns in the planetary-scale field in the Greenland, EAE and Ural regions, we have not given any attention to the physical mechanism of the genesis of Euro–Atlantic blocking events and their variability in intensity, location and duration. More recently, Masato et al. (2012) found that cold-cyclonic (warm-anticyclonic) wave breaking, referred to as CCWB (WAWB), takes place mainly over the oceanic basin (Europe). Thus, the SW–NE (SE–NW) oriented dipole-type block over the Greenland (Ural) region in Fig. 10a (10c) is, to a large extent, closely related to CCWB (WAWB). However, different from previous investigations, our study provides another explanation as to why there are preferable SW–NE- and SE–NW-oriented dipole-type blocks in a planetary-scale field over the Greenland and Ural regions as well as Ω-type blockings over the EAE region.

7. Discussion and conclusion

In this paper, we have investigated, from observational and theoretical viewpoints, why the planetary-scale fields of intense and long-lived blocking events can have three different flow patterns in the Greenland, EAE and Ural regions. We found that the occurrence position of Euro–Atlantic blocking events is dominated by the existence region of the weak westerly wind of the North Atlantic jet stream. The composite fields of intense or long-lived blocking events exhibit SW–NE- and SE–NW-oriented dipole-type blocks in the Greenland and Ural regions, respectively, whereas an Ω-type blocking is evident over the EAE region.

Moreover, the physical cause of the different blocking flow pattern in the different sub-regions can be explained in terms of an NMI model developed by Luo (2005) and Luo and Cha (2012). In this model, the planetary-scale field of a blocking event is constructed as a superposition of the blocking dipole anomaly and the CSW anomaly with a monopole meridional pattern. It is found that for a fixed storm track strength the longitudinal position of the blocking dipole anomaly relative to the positive CSW anomaly is crucial for what types of blocking patterns the planetary-scale fields of intense or long-lived blocking events can have in the Greenland, EAE and Ural regions. Over the EAE region because the blocking dipole anomaly is within a position

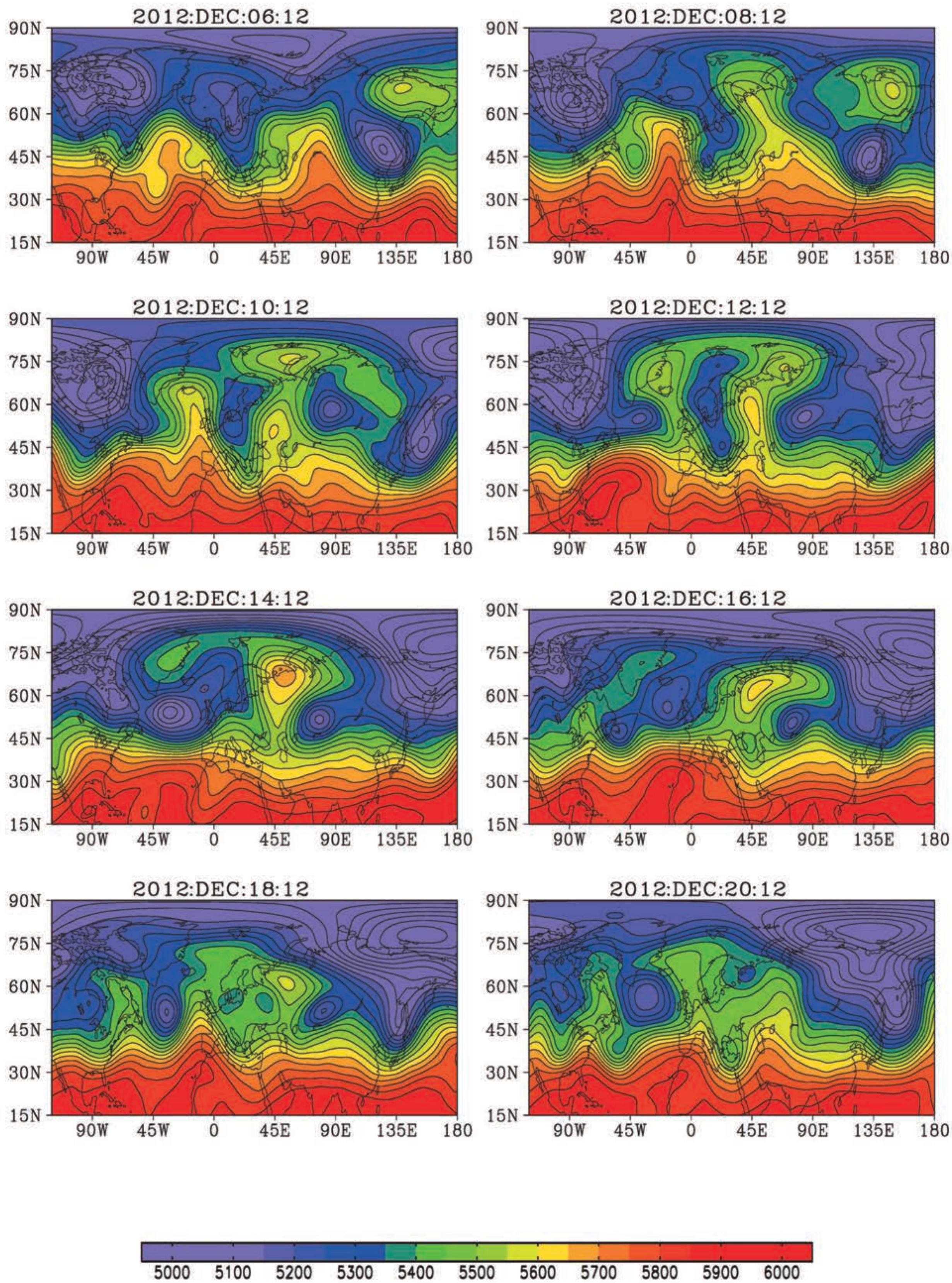

Fig. 9. Instantaneous 500-hPa geopotential height fields of a blocking event occurring in the period 6–20 Dec 2012 over the European continent. Units: m.

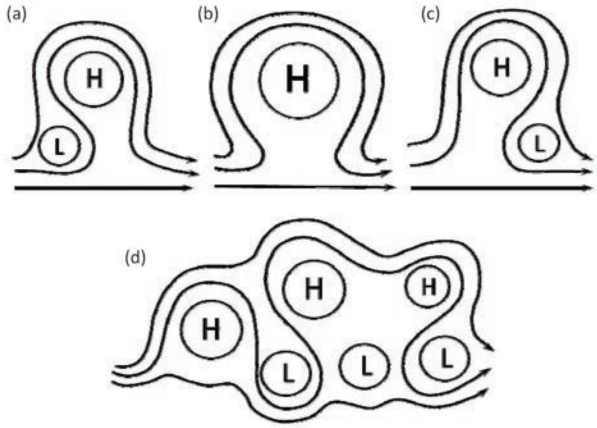

Fig. 10. Schematic representations of the flow patterns of winter blocking events in the Euro–Atlantic sector: (a) southwest–northeast-oriented dipole-type pattern; (b) Ω-type pattern; (c) southeast–northwest-oriented dipole-type pattern; and (d) Berggren–Bolin–Rossby meandering jet type.

almost the same as the positive CSW anomaly, the planetary-scale field of the eddy-driven blocking can exhibit an Ω-type blocking pattern. However, over the Greenland and Ural regions, because the blocking dipole anomaly is farther in the west (east) of the positive CSW anomaly and undergoes a retrogression, a SW–NE (SE–NW) oriented dipole block can be seen. Of course, when the Atlantic storm track is particularly intense, or when the mean zonal wind is particularly weak in the three regions, the blocking dipole anomaly becomes particularly strong so that the planetary-scale field can still exhibit a dipole-type block pattern. Nevertheless, such blocking cases may be rare.

Although the theoretical results obtained here are based on a simplified barotropic model, they can still capture the essence of observed blocking patterns. Of course, a study of many problems such as a quantitative comparison with a complicated model is needed in future work.

Acknowledgements. The authors acknowledge the support from the National Science Foundation of China (Grant No. 41375067) and "One-Hundred Talents Plan" of the Chinese Academy of Sciences (Grant No. Y163011).

REFERENCES

Barriopedro, D., R. Garcia-Herrera, A. R. Lupo, and E. Hernández, 2006: A climatology of Northern Hemisphere blocking. *J. Climate*, **19**, 1042–1063.

Benedict, J. J., L. Sukyoung, and S. B. Feldstein, 2004: Synoptic view of the North Atlantic Oscillation. *J. Atmos. Sci.*, **61**, 121–144.

Berggren, R., B. Bolin, and C.-G. Rossby, 1949: An aerological study of zonal motion, its perturbations and break-down. *Tellus*, **1**, 14–37.

Buehler, T., C. C. Raible, and T. F. Stocker, 2011: The relationship of winter season North Atlantic blocking frequencies to extreme cold or dry spells in the ERA-40. *Tellus A*, **63**, 212–222.

Cattiaux, J., R. Vautard, C. Cassou, P. Yiou, V. Masson-Delmotte, and F. Codron, 2010: Winter 2010 in Europe: A cold extreme in a warming climate. *Geophys. Res. Lett.*, **37**, L20704, doi: 10.1029/2010GL044613.

Charney, J. G., and J. G. DeVore, 1979: Multiple flow equilibria in the atmosphere and blocking. *J. Atmos. Sci.*, **36**, 1205–1216.

Cheung, H. N., W. Zhou, H. Y. Mok, and M. C. Wu, 2012: Relationship between Ural-Siberian blocking and the East Asian Winter Monsoon in relation to the Arctic Oscillation and the El Nino-Southern Oscillation. *J. Climate*, **25**, 4242–4257.

Cheung, H. N., W. Zhou, Y. P. Shao, W. Chen, H. Y. Mok, and M. C. Wu, 2013: Observational climatology and characteristics of wintertime atmospheric blocking over Ural-Siberia. *Climate Dyn.*, **41**, 63–79.

Colucci, S. J., 1985: Explosive cyclogenesis and large-scale circulation changes: Implications for atmospheric blocking. *J. Atmos. Sci.*, **42**, 2701–2717.

Davini, P., C. Cagnazzo, S. Gualdi, and A. Navarra, 2012a: Bidimensional diagnostics, variability and trends of Northern Hemisphere blocking. *J. Climate*, **25**, 6496–6509.

Davini, P., C. Cagnazzo, R. Neale, and J. Tribbia, 2012b: Coupling between Greenland blocking and the North Atlantic Oscillation pattern. *Geophys. Res. Lett.*, **39**, l14701, doi: 10.1029/2012GL052315.

de Vries, H., R. J. Haarsma, W. Hazeleger, 2012: Western European cold spells in current and future climate. *Geophys. Res. Lett.*, **39**, L04706, doi: 10.1029/2011GL050665.

Diao, Y., J. Li, and D. Luo, 2006: A new blocking index and its application: Blocking action in the Northern Hemisphere. *J. Climate*, **19**, 4819–4839.

Dole, R. M., and Coauthors, 2011: Was there a basis for anticipating the 2010 Russian heat wave? *Geophys. Res. Lett.*, **38**, L06702, doi: 10.1029/2010GL046582.

Franzke, C., S. Lee, and S. B. Feldstein, 2004: Is the North Atlantic Oscillation a breaking wave? *J. Atmos. Sci.*, **61**, 145–160.

Green, J. S. A., 1977: The weather during July 1976: Some dynamical considerations of the drought. *Weather*, **32**, 120–126.

Haines, K., and J. C. Marshall, 1987: Eddy-forced coherent patterns as a prototype of atmospheric blocking. *Quart. J. Roy. Meteor. Soc.*, **113**, 681–704.

Higgins, R. W., and S. D. Schubert, 1994: Simulated life cycles of persistent anticyclonic anomalies over the North Pacific: Role of synoptic-scale eddies. *J. Atmos. Sci.*, **51**, 3238–3259.

Holopainen, E., and C. Fortelius, 1987: High-frequency transient eddies and blocking. *J. Atmos. Sci.*, **44**, 1632–1645.

Lejenäs, H., and H. Økland, 1983: Characteristics of northern hemisphere blocking as determined from a long time series of observational data. *Tellus A*, **35A**, 350–362, doi: 10.1111/j.1600–0870.1983.tb00210.x.

Luo, D., 2005: A barotropic envelope Rossby soliton model for block-eddy interaction. Part I: Effect of topography. *J. Atmos. Sci.*, **62**, 5–21.

Luo, D., and J. Cha, 2012: The North Atlantic Oscillation and the North Atlantic jet variability: Precursors to NAO regimes and transitions. *J. Atmos. Sci.*, **69**, 3764–3787.

Masato, G., B. J. Hoskins, and T. J. Woollings, 2012: Wave-breaking characteristics of midlatitude atmospheric blocking. *Quart. J. Roy. Meteor. Soc.*, **138**, 1285–1296.

McWilliams, J. C., 1980: An application of equivalent modons to atmospheric blocking. *Dyn. Atmos. Oceans*, **5**, 43–66.

Nakamura, H., and J. M. Wallace, 1993: Synoptic behavior of baroclinic eddies during the blocking onset. *Mon. Wea. Rev.*, **121**, 1892–1903.

Pelly, J. L., and B. J. Hoskins, 2003: A new perspective on blocking. *J. Atmos. Sci.*, **60**, 743–755.

Rex, D. F., 1950a: Blocking action in the middle troposphere and its effect upon regional climate. I. An aerological study of blocking action. *Tellus*, **2**, 196–211.

Rex, D. F., 1950b: Blocking actions in the middle troposphere and its effects upon regional climate. II: The climatology of blocking action. *Tellus*, **2**, 275–301.

Shutts, G. J., 1983: The propagation of eddies in diffluent jet streams: Eddy vorticity forcing of blocking flow fields. *Quart. J. Roy. Meteor. Soc.*, **109**, 737–761.

Sillmann, J., M. Croci-Maspoli, M. Kallache, and R, W. Katz, 2011: Extreme cold winter temperatures in Europe under the influence of North Atlantic atmospheric blocking. *J. Climate*, **24**, 5899–5913.

Sung, M. K., G. H. Lim, J. S. Kug, and S. An, 2011: A linkage between the North Atlantic Oscillation and its downstream development due to the existence of a blocking ridge. *J. Geophys. Res.*, **116**, doi: 10.1029/2010JD015006.

Tibaldi, S., and F. Molteni, 1990: On the operational predictability of blocking. *Tellus*, **42A**, 343–365.

Tyrlis, E., and B. J. Hoskins, 2008: Aspects of a northern hemisphere atmospheric blocking climatology. *J. Atmos. Sci.*, **65**, 1638–1652.

Trigo, R. M., R. García-Herrera, J. Díaz, I. F. Trigo, and M. A. Valente, 2005: How exceptional was the early August 2003 heatwave in France? *Geophys. Res. Lett.*, **32**, L10701, doi: 10.1029/2005GL022410.

White, W.B. and N. E. Clark, 1975: Development of Blocking Ridge Activity over Central North Pacific. *J. Atmos. Sci.*, **32**, 489-502.

Wiedenmann, J. M., A. R. Lupo, I. I. Mokhov, and E. Tikhonova, 2002: The climatology of blocking anticyclones for the Northern and Southern Hemispheres: Block intensity as a diagnostic. *J. Climate*, **15**, 3459–3473.

Woollings, T. J., B. J. Hoskins, M. Blackburn, and P. Berrisford, 2008: A new Rossby wave-breaking interpretation of the North Atlantic Oscillation. *J. Atmos. Sci.*, **65**, 609–626.

Yamazaki, A., and H. Itoh, 2013: Vortex–vortex interactions for the maintenance of blocking. Part I: The selective absorption mechanism and a case study. *J. Atmos. Sci.*, **70**, 725–742.